A Novel Primer to Prevent Nanoparticle Agglomeration in Mixed Matrix Membranes

Yi Li, William B. Krantz, and Tai-Shung Chung
Dept. of Chemical and Biomolecular Engineering, National University of Singapore,
10 Kent Ridge Crescent, Singapore 119260

DOI 10.1002/aic.11239
Published online July 27, 2007 in Wiley InterScience (www.interscience.wiley.com).

Keywords: nanoparticle agglomeration, Interface quality, mixed matrix membranes, sulfonated poly(ether sulfone), priming method

Introduction

During the past two decades, polymer-based organic-inorganic composites have received world-wide attention in the field of materials science. This is because the resultant materials can offer superior performance in terms of mechanical toughness for engineering resins, permeability and selectivity for gas/liquid separation, and photoconductivity for electronics.[1–3] After the discovery by researchers at UOP LLC on mixed matrix membranes (MMMs),[4] this new concept has also been applied to the membrane-based gas/liquid separations by combining the easy processability of polymeric materials, with the excellent separation properties of inorganic materials.[5,6] The poor compatibility between the polymer matrix and inorganic particles, which has been a major obstacle to the development of MMMs,[7,8] has been improved significantly through some methods, such as the silane modification on the particle surface,[9,10] the introduction of a compatibility agent between the polymer matrix and inorganic particles,[11] and the application of high-processing temperatures during the membrane formation.[12,13] However, the aforementioned MMM studies focused on the formation of flat dense membranes. Flat-dense MMMs can provide the intrinsic properties of this type of organic-inorganic composite material for academic research; however, they are not appropriate for industrial applications due to their much thicker dense-selective layer and substantially lower gas-permeation flux.

In the last 20 years, the asymmetric hollow-fiber membrane has become a favored configuration for membrane-based gas separation systems due to its many advantages.[14,15] Therefore, it would be a significant advance if polymer-based organic-inorganic composite materials could be incorporated a hollow-fiber membrane configuration for gas separation. Pioneering progress toward this end has been made through the utilization of dual-layer hollow fibers.[16–19] Dual-layer hollow-fiber membranes formed by coextrusion represent a breakthrough in hollow-fiber fabrication technology.[20] They basically consist of an asymmetric separating outer layer and a microporous supporting inner layer. One could efficiently lower the fabrication cost and easily control the distribution of inorganic particles by using organic-inorganic composite materials only in the thin outer layer. Through continuous progress in developing the coextrusion technology, Chung and coworkers have successfully fabricated dual-layer hollow-fiber membranes with a mixed matrix dense-selective layer thickness of 5.5×10^{-7} m (0.55 μm), while retaining the superior separation performance of mixed matrix materials.[18] This is the thinnest selective layer reported to date for dual-layer hollow-fiber membranes made from mixed matrix materials. However, in order to potentially replace the hollow-fiber membranes made from just polymeric materials, dual-layer hollow fiber membranes with a mixed matrix dense-selective layer thickness of 1×10^{-7} m (0.1 μm) are highly desirable. Regrettably, the further reduction in the mixed matrix dense-selective layer thickness is restricted by both the size and the agglomeration of the inorganic nanoparticles currently available.

To date, most of MMM studies have used rather large inorganic particles 0.3–5 $\times 10^{-6}$ m (0.3–5 μm). This is mainly due to the fact that more severe agglomeration occurs in the polymer matrix when smaller particles are used, especially at high-particle loadings. The agglomeration of nanoparticles with a size of less than 1×10^{-7} m (100 nm) has significantly impeded their application in developing the practical mixed matrix hollow-fiber membranes. This is because the agglomeration is thought to be responsible for defects among the par-

Correspondence concerning this article should be addressed to T.-S. Chung at chencts@nus.edu.sg.

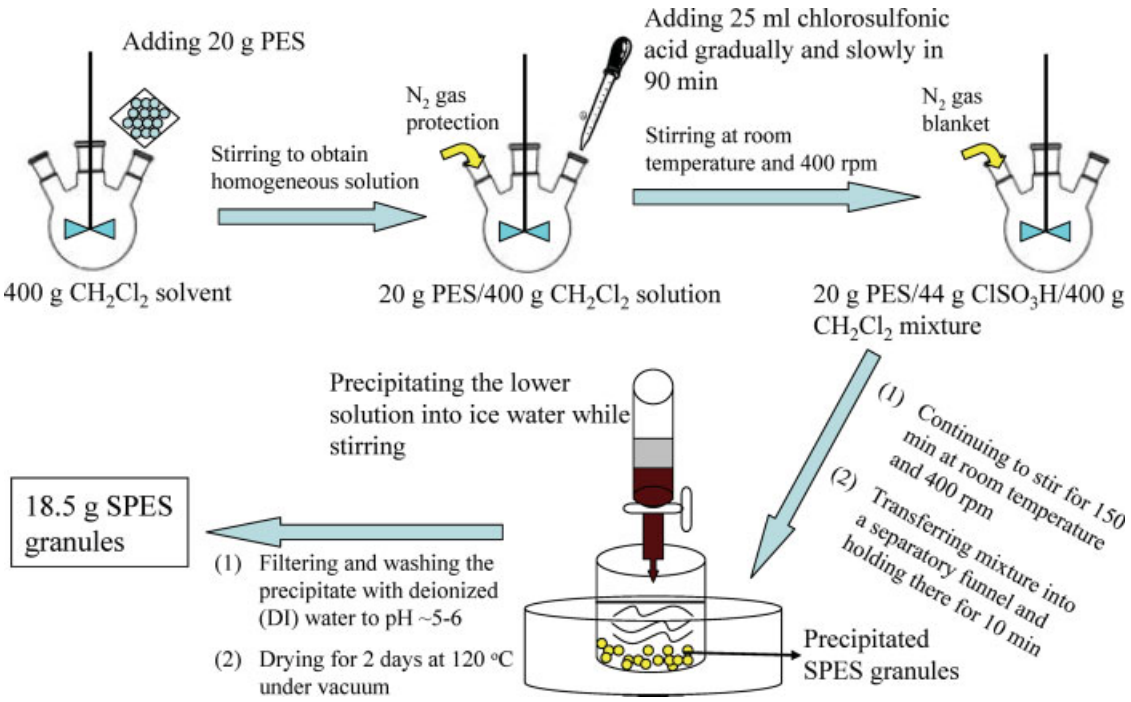

Figure 1. Flow chart for the PES sulfonation reaction.

[Color figure can be viewed in the online issue, which is available at www.interscience.wiley.com.]

ticles and/or between the polymer matrix and particle phases. Therefore, the purpose of this communication is to propose a novel primer-sulfonated poly(ether sulfone) (SPES) to prevent nanoparticle agglomeration, and improve the interface quality between polymer and particle phases in MMMs. To the best of our knowledge, there have been no prior publications on using SPES polymer to prime the surface of nanoparticles to inhibit their agglomeration.

Self-synthesized zeolite 4A with an average size of 1×10^{-7} m (100 nm) was selected as the dispersed phase, due to its suitable pore size for gas separation,[10,12,13] while poly(ether sulfone) (PES) was chosen as the continuous polymer matrix because of its appropriate glass-transition temperature (T_g) of 215 °C and various applications in gas separations.[21] The SPES polymer was characterized by acid-base titration, elemental analysis and X-ray photoelectron spectroscopy (XPS). Flat-dense PES-zeolite 4A MMMs were fabricated, based on a relatively straightforward approach by applying a high-processing temperature during the membrane formation.[10,12,13] The gas-permeation rates of PES-zeolite 4A MMMs were measured as a function of SPES priming. The morphology of these newly developed MMMs was characterized via scanning electron microscopy (SEM).

Experimental

Materials

A commercial Radel® A PES was obtained from Solvay Advanced Polymers L.L.C., Georgia, USA, and was dried at 120 °C overnight *in vacuo* before use. N-methyl-2-pyrrolidone (NMP), dichloromethane and chlorosulfonic acid were purchased from Merck. NMP was dried using the activated molecular sieve 4A beads, with a diameter of 0.003–0.005 m (3-5 mm) supplied by Research Chemicals, Ltd., and then filtered through a 2×10^{-7} m (0.2 μm) Teflon filter before use, whereas dichloromethane and chlorosulfonic acid were used without further purification. Zeolite 4A synthesized in our laboratory was used as the inorganic phase in the MMMs; its average particle size was around 1×10^{-7} m (100 nm) as determined by SEM. To remove the adsorbed water vapor or other organic vapors, zeolite 4A was dehydrated at 250 °C for 7,200 s (2 h) *in vacuo* before use.

PES sulfonation procedure

Figure 1 shows the flow chart of the PES sulfonation reaction used in this study. This procedure was developed with some modification from other work.[22,23] The nitrogen protection inhibits any side reactions resulting from the fast decomposition of chlorosulfonic acid in the atmosphere.

Preparation procedure of polymer-zeolite MMMs

Since the fabrication method of flat-dense MMMs developed in our prior studies has displayed good properties,[13] the same method involving "high-processing temperatures during the membrane formation" was employed in this work, with only one difference. In our prior studies, a small amount of PES was used as a primer to enhance the compatibility between the polymer and zeolite phases before adding the PES bulk, whereas in this work, SPES was used to substitute PES as the primer to improve the zeolite dispersion. The flow chart of the preparation procedure for the PES-zeolite 4A MMMs is illustrated in Figure 2. The resultant dried flat-dense MMMs have

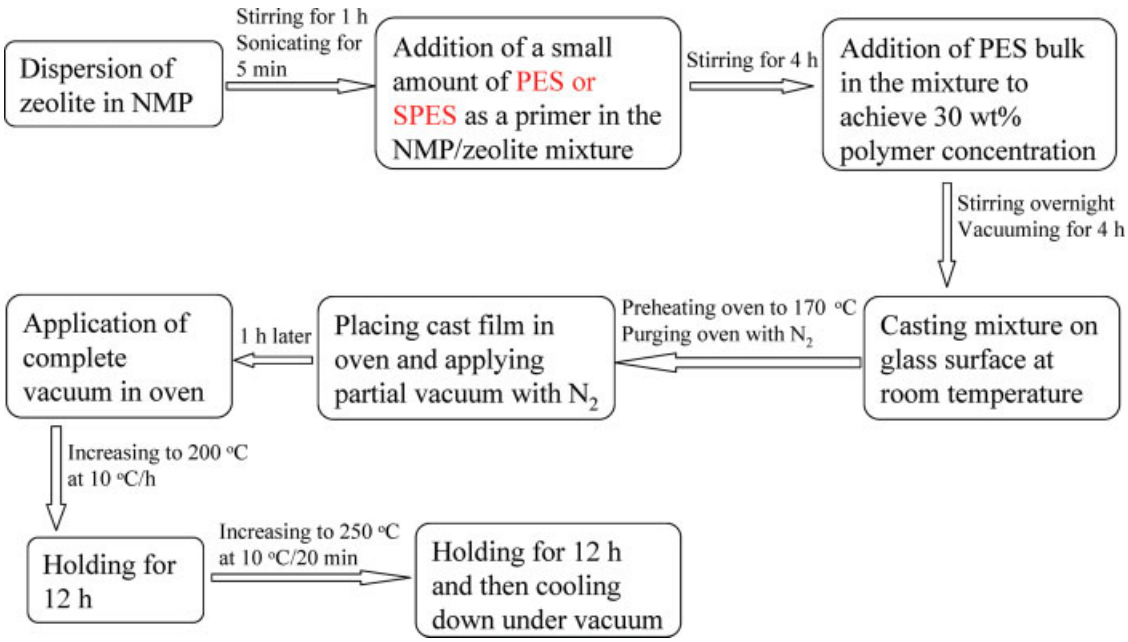

Figure 2. Flow chart for the preparation procedure of PES-zeolite 4A MMMs.

[Color figure can be viewed in the online issue, which is available at www.interscience.wiley.com.]

thicknesses varying from 50 μm to 60 μm for the permeability measurement.

Gas permeability measurement

The gas permeation properties of MMMs were measured using the variable-pressure constant-volume method with a precalibrated permeation cell described elsewhere.[24] Each pure gas was tested in the sequence of He, H_2, O_2, N_2, CH_4 and CO_2, and replicated three times for each membrane. The measurement of H_2 gas for MMMs was performed at 35 °C and 3.5464×10^5 Pa (3.5 atm); the measurement of the other gases was conducted at 35 °C and 1.01325×10^6 Pa (10 atm).

Other characterization

After the PES sulfonation reaction, the degree of sulfonation (DS) and ion-exchange capacity (IEC) of the SPES polymer were determined via acid-base titration, which has been defined in detail in prior work.[23] In brief, a known amount of dry SPES polymer was dissolved in the solvent, and the discharged H^+ amount was measured using a standard sodium hydroxyl solution and a phenolphthalein indicator.

Two analytical methods were also used to qualitatively determine whether the PES sulfonation reaction had taken place. The first was elemental analysis using a PerkinElmer PE 2400 Series II CHNS/O analyzer. The second was X-ray photoelectron spectroscopy (XPS) conducted on a Shimadzu ESCAKL spectrometer using a nonmonochromatic Mg Kα photon source.

The electron micrographs of the MMM morphology were examined by SEM on a JEOL JSM-5600LV and JSM-6700F, to compare the differences in the dispersion of the zeolite particles and interface quality between two phases before and after using SPES polymer as a primer.

Results and Discussion

SPES polymer with a DS value of 62.1 wt % and an IEC value of 1.40 eq/kg (1.40 mequiv/g) was obtained by the PES sulfonation reaction in this work. DS and IEC values of the SPES polymer were determined via acid-base titration, which has been defined in detail in prior work.[23] The results for its characterization via elemental analysis and XPS are summarized in Table 1. By comparing these results with those for the PES polymer, it can be seen that more oxygen and sulfur content are detected in the SPES polymer, thus, confirming that the sulfonic group (SO_3H) has been attached to the polymer backbone chains.

Figure 3 shows the comparison of cross-sectional SEM images of flat-dense PES-zeolite 4A MMMs with 20 wt % zeolite loading between using PES as a primer (left column), and using SPES as a primer (right column). It can be easily seen that if using PES as a primer, there are many large agglomerations distributing in the whole cross-section due to the incompatibility between the PES matrix and zeolite phases. However, using SPES as a primer not only effectively prevents the agglomeration of nanoscale zeolite particles (1×10^{-7} m (100 nm)), thereby, obtaining good zeolite dispersion, but also significantly improves the contact between the polymer matrix and zeolite phases, thus, leading to an excellent interface quality in the MMMs. When the SPES polymer is used as a primer, the excellent interface quality between PES and zeolite phases might result from the fact that the SPES polymer becomes hydrophilic due to the attachment of the sulfonic group, thereby, resulting in a strong interaction (i.e., hydrogen bonding) with hydrophilic zeolite 4A; however, the SPES polymer still possesses a good affinity with the PES matrix due to their having similar backbone chains. On the other hand, the good zeolite dispersion might be due to the fact that the sulfonic

Table 1. Comparison of Weight Percentages of Various Elements in PES and SPES Polymers Measured by Elemental Analysis and XPS

	Elemental Analysis*		XPS**	
	PES Polymer	SPES Polymer	PES Polymer	SPES Polymer
C (wt%)	63.8	57.3	66.5	58.2
O (wt%)	20.4	24.8	20.5	25.3
S (wt%)	12.0	14.8	13.0	16.5
H (wt%)	3.80	3.10		

*The weight percentages of oxygen shown in the column for elemental analysis were calculated by 100%-C%-S%-H% because the elemental analysis results did not give the oxygen content.
**The weight percentages of elements shown in the column for XPS did not include hydrogen in the calculation because XPS could not detect hydrogen.

group of the SPES polymer carries negative charges after the H^+ dissociation in the solvent, and accordingly, the zeolite particles repel each other after priming a thin SPES layer on them due to the electrostatic interaction.

The morphology change of flat-dense PES-zeolite 4A MMMs with 20 wt % zeolite loading after using SPES polymer as a primer is demonstrated by their gas separation performance shown in Table 2. The pure polymer PES dense film was also prepared using the same procedure as used for the MMM fabrication for comparison. When using the PES polymer as a primer, the PES-zeolite 4A MMMs display high O_2 and N_2 permeabilities, while their O_2/N_2 selectivity is poor and follows Knudsen diffusion. This might be because as illustrated in Figure 3, the serious agglomeration of zeolite nanoparticles and incompatibility between the PES matrix and zeolite phases might cause many defects among the nanoparticles and between the PES matrix and particles, thus, forming a continuous pathway for Knudsen diffusion. When using SPES as a primer, the gas-separation performance of PES-zeolite 4A MMMs is dominated by the sorption-diffusion mechanism, thus, verifying that the defects induced by the nanoparticle agglomeration and poor interface quality have been completely eliminated through the application of SPES primer. When compared with the pure polymer PES dense film, the PES-zeolite 4A MMMs with a primer of SPES present a lower permeability for all tested gases, as well as an enhanced selectivity. The reduction in the gas permeability is easily understandable, because it has been previously demonstrated that both polymer chain rigidification and partial pore blockage of zeolites can lead to a decrease in the permeability of MMMs.[10,12,13,25] The enhancement in the gas pair selectivity is easily explainable due to the influence of the molecular sieving mechanism provided by the zeolite, however, the extent of enhancement may be impaired by the partial pore blockage of zeolites resulting from the attachment of polymer chains, because the pore size of zeolite 4A is very close to the O_2 and N_2 molecular kinetic diameters, which has been discussed extensively in the other related work.[10,12,13,25]

To evaluate the effectiveness of SPES as a primer in preventing the nanoparticle agglomeration and improving the interface

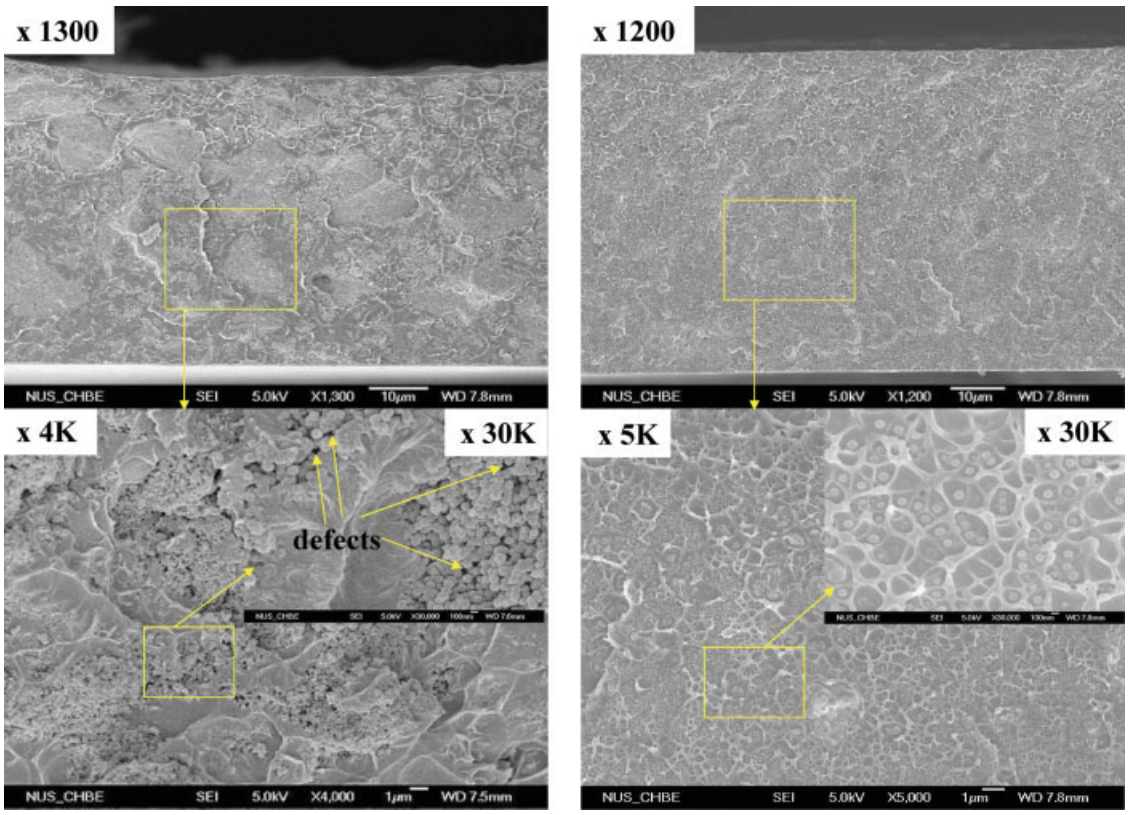

Figure 3. Comparison of cross-sectional SEM images of PES-zeolite 4A MMMs with different primers at 20 wt % zeolite loading (left: PES as a primer; right: SPES as a primer; inset: high magnification images).

[Color figure can be viewed in the online issue, which is available at www.interscience.wiley.com.]

Table 2. Comparison of Gas Separation Performance of Flat-Dense PES-Zeolite 4A MMMs using PES or SPES as a Primer at 20 wt % Zeolite Loading

	Permeability (Barrer*)						Ideal Selectivity			
	He	H_2	O_2	N_2	CH_4	CO_2	P(He)/P(N_2)	P(H_2)/P(N_2)	P(O_2)/P(N_2)	P(CO_2)/P(CH_4)
Pure polymer PES dense film	7.22	6.45	0.479	0.0825	0.0841	2.64	87.5	78.2	5.81	31.4
PES-zeolite 4A MMMs using PES as a primer			471	503					0.936	
PES-zeolite 4A MMMs using SPES as a primer	6.67	5.82	0.406	0.0640	0.0541	1.75	104.2	90.9	6.34	32.3

*1 Barrer = 7.5005×10^{-18} m^2 s^{-1} Pa^{-1}.

quality at a higher particle loading, PES-zeolite 4A MMMs with 40 wt % zeolite loading were fabricated by the same method as the MMMs with 20 wt % zeolite loading and characterized by SEM. As shown in the left column of Figure 4, the noticeable agglomeration and the poor interface quality indicate the ineffectiveness of SPES as a primer for MMMs with a higher particle loading. However, after some consideration, it is conjectured that this phenomenon might result from an insufficient SPES amount used in the fabrication of the MMMs, with a higher particle loading, rather than from the SPES itself. The amount of SPES polymer used in this study in the fabrication of the MMMs with both 20 and 40 wt % zeolite loadings was initially set to 10 wt % of the total polymer solid amount. It can be seen that the weight ratios of SPES to nanoscale zeolite 4A decreased from 0.40 to 0.15, when the zeolite loading increased from 20 to 40 wt %, because the amount of the total polymer solid used was kept constant irrespective of the zeolite loading. The deficiency of SPES polymer at a higher zeolite loading might not provide a sufficient priming layer on the zeolite surface, thus, resulting in the apparent nanoparticle agglomeration and the undesirable interface quality. Therefore, another sample of PES-zeolite 4A MMM with 40 wt % zeolite loading was prepared by the same method with one substantial difference: the weight ratio value of SPES to zeolite 4A was kept at 0.40. It can be seen that excellent zeolite dispersion and interface quality are displayed in the right column of Figure 4, which demonstrates the effectiveness of SPES as a primer even at a higher particle loading if the weight ratio of the SPES to zeolite 4A is kept constant (e.g., 0.40 in this study).

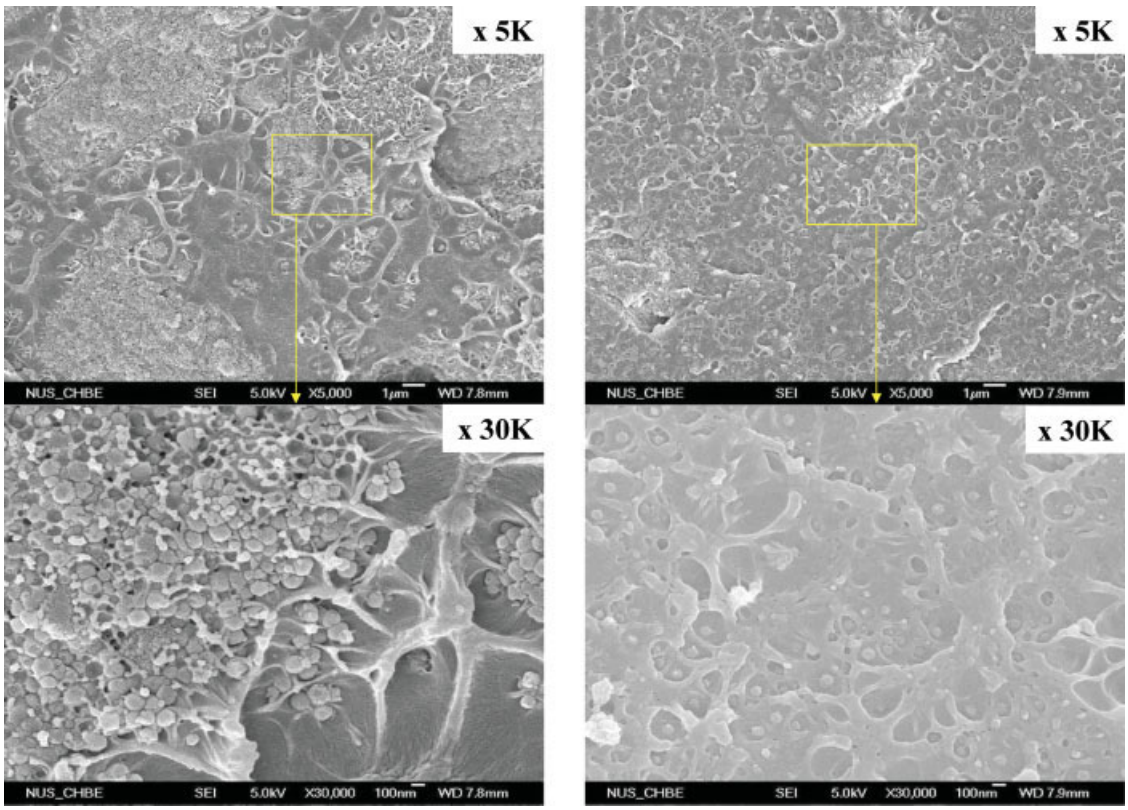

Figure 4. Comparison of cross-sectional SEM images of PES-zeolite 4A MMMs with different weight ratios of SPES to zeolite 4A at 40 wt % zeolite loading (left: 0.15; right: 0.40).

[Color figure can be viewed in the online issue, which is available at www.interscience.wiley.com.]

Conclusions

A novel primer of SPES polymer has been found for fabricating PES-zeolite 4A MMMs. Compared with PES as a primer, SEM images show that the SPES primer can not only effectively prevent the nanoparticles from agglomerating by providing electrostatic repulsion via the sulfonic groups on the SPES polymer, but also provide an exceptional improvement in the interface quality between polymer matrix and zeolite phases by forming the strong interaction with both the PES matrix and zeolite 4A. The change in the gas separation mechanism of MMMs from Knudsen diffusion to sorption-diffusion demonstrates that the defects induced by the nanoparticle agglomeration and poor interface quality have been completely eliminated through the application of the SPES primer. Even at a high-particle loading (e.g., 40 wt %), the SPES polymer still performs well as a primer if the weight ratio of SPES to particles is kept at an appropriate constant.

Acknowledgments

The authors would like to thank NUS and A*STAR for funding this research via grant numbers R-279-000-184-112, R-279-000-164-305 and R-398-000-029-305 and Solvay Advanced Polymers L.L.C for providing the PES polymer.

Literature Cited

1. Peng GW, Qiu F, Ginzburg VV, Jasnow D, Balazs AC. Forming supramolecular networks from nanoscale rods in binary, phase-separating mixtures. *Science*. 2000;288:1802–1804.
2. Merkel TC, Freeman BD, Spontak RJ, He Z, Pinnau I, Meakin P, Hill AJ. Ultrapermeable, reverse-selective nanocomposite membranes. *Science*. 2002;296:519–522.
3. Wang Y, Herron N. X-ray photoconductive nanocomposites. *Science*. 1996;273:632–634.
4. Kulprathipanja S, Neuzil RW, Li NN. Separation of fluids by means of mixed matrix membranes in gas permeation. US Patent No. 4,740,219; 1988.
5. Jia MD, Peinemann KV, Behling RD, Molecular sieving effect of the zeolite-filled silicone rubber membranes in gas permeation. *J Membr Sci*. 1991;57:289–296.
6. Mahajan R, Koros WJ. Factors controlling successful formation of mixed-matrix gas separation materials. *Ind Eng Chem Res*. 2000;39: 2692–2696.
7. Süer MG, Baç N, Yilmaz L. Gas permeation characteristics of polymer-zeolite mixed matrix membranes. *J Membr Sci*. 1994;91:77–86.
8. Mahajan R, Burns R, Schaeffer M, Koros WJ. Challenges in forming successful mixed matrix membranes with rigid polymeric materials. *J App Polym Sci*. 2002;86:881–890.
9. Liu YL, Su YH, Lee KR, Lai JY. Crosslinked organic-inorganic hybrid chitosan membranes for pervaporation dehydration of isopropanol-water mixtures with a long-term stability. *J Membr Sci*. 2005;251:233–238.
10. Li Y, Guan HM, Chung TS, Kulprathipanja S. Effects of novel silane modification of zeolite surface on polymer chain rigidification and partial pore blockage in polyethersulfone (PES)-zeolite A mixed matrix membranes. *J Membr Sci*. 2006;275:17–28.
11. Yong HH, Park HC, Kang YS, Won J, Kim WN. Zeolite-filled polyimide membrane containing 2,4,6-triaminopyrimidine. *J Membr Sci*. 2001;188:151–163.
12. Mahajan R. Formation, characterization and modeling of mixed matrix membrane materials. The University of Texas at Austin, 2000. PhD. Dissertation.
13. Li Y, Chung TS, Cao C, Kulprathipanja S. The effects of polymer chain rigidification, zeolite pore size and pore blockage on polyethersulfone (PES)-zeolite A mixed matrix membranes. *J Membr Sci*. 2005; 260:45–55.
14. Chung, TS. A review of microporous composite polymeric membrane technology for air-separation. *Polym Polym Comp*. 1996;4:269–283.
15. Wang KY, Matsuura T, Chung TS, Guo WF. The effects of flow angle and shear rate within the spinneret on the separation performance of poly(ethersulfone) (PES) ultrafiltration hollow fiber membranes. *J Membr Sci*. 2004;240:67–79.
16. Jiang LY, Chung TS, Cao C, Huang Z, Kulprathipanja S. Fundamental understanding of nano-sized zeolite distribution in the formation of the mixed matrix single- and dual-layer asymmetric hollow fiber membranes. *J Membr Sci*. 2005;252:89–100.
17. Jiang LY, Chung TS, Kulprathipanja S. An investigation to revitalize the separation performance of hollow fibers with a thin mixed matrix composite skin for gas separation. *J Membr Sci*. 2006;276:113–125.
18. Li Y, Chung TS, Huang Z, Kulprathipanja S. Dual-layer polyethersulfone (PES)/BTDA-TDI/MDI co-polyimide (P84) hollow fiber membranes with a submicron PES-zeolite beta mixed matrix dense-selective layer for gas separation. *J Membr Sci*. 2006;277:28–37.
19. Jiang LY, Chung TS, Kulprathipanja S. A novel approach to fabricate mixed matrix hollow fibers with superior intimate polymer/zeolite interface for gas separation. *AIChE J*. 2006;52:2898–2908.
20. Ekiner OM, Hayes RA, Manos P. Novel multicomponent fluid separation membranes. US Patent No. 5,085,676, 1992.
21. Chiou JS, Maeda Y, Paul DR. Gas permeation in polyethersulfone. *J App Polym Sci*. 1987;33:1823–1828.
22. Pu T, Zeng ZX. Preparation method of sulfonated polyethersulfone. Chinese Patent No. CN1267676A, 2000.
23. Guan R, Zou H, Lu D, Gong C, Liu Y. Polyethersulfone sulfonated by chlorosulfonic acid and its membrane characteristics. *Eur Polym J*. 2005;41:1554–1560.
24. Lin WH, Vora RH, Chung TS. Gas transport properties of 6FDA-Durene/1,4-phenylenediamine (pPDA) copolyimides. *J Polym Sci Polym Phys*. 2000;38:2703–2713.
25. Li Y, Chung TS, Kulprathipanja S. Novel Ag^+-zeolite/polymer mixed matrix membranes with a high CO_2/CH_4 selectivity. *AIChE J*. 2007;53:610–616.

Manuscript received Feb. 15, 2007, and revision received Apr. 27, 2007.